

## Research Article

# Research on Dynamic Monitoring and Early Warning of the High-Rise Building Machine during the Climbing Stage

Xi Pan <sup>1,2</sup>, Zibo Zuo <sup>2,3</sup>, Longlong Zhang <sup>2</sup> and Tingsheng Zhao<sup>1</sup>

<sup>1</sup>School of Civil and Hydraulic Engineering, Huazhong University of Science and Technology, Wuhan, Hubei 430074, China

<sup>2</sup>General Engineering Institute of Shanghai Construction Group, Shanghai Construction Group Co. Ltd., Shanghai 200080, China

<sup>3</sup>Department of Structural Engineering and Building Materials, Faculty of Engineering and Architecture, Ghent University, Ghent 9000, Belgium

Correspondence should be addressed to Zibo Zuo; zuozibo@hotmail.com

Received 24 December 2022; Revised 19 August 2023; Accepted 13 October 2023; Published 31 October 2023

Academic Editor: Afaq Ahmad

Copyright © 2023 Xi Pan et al. This is an open access article distributed under the Creative Commons Attribution License, which permits unrestricted use, distribution, and reproduction in any medium, provided the original work is properly cited.

High-rise building machines (HBMs) are commonly used for the construction of super-high skyscrapers. Monitoring and early warning are critical to ensure the safety of giant HBMs during dynamic climbing. However, no indicators or control methods directly reflect the dynamic safety state of such large structures. In this study, the key factors influencing the climbing altitude were systematically analyzed and a method for the dynamic monitoring and early warning of HBMs during climbing was proposed. This approach is innovative for monitoring 3D attitude in real time using a string of fiber grating-level sensors mounted on the main bearing surface of the HBM. Three-level early warning indicators and control methods that reflect the safety status of the HBM during dynamic climbing have been established. The method was successfully applied to a 356-m tall high-rise project, the Shenzhen Xinghe Yabao Building. Results demonstrate that the proposed method can monitor and control the safety state of the HBM climbing process more accurately than current methods in real time. In addition, it significantly reduces the impact of factors such as preclimbing differential deformation and climbing attitude recognition on the accuracy of the HBM climbing control. This guarantees the safe management of HBMs and the efficient construction of super high-rise buildings. The results of this study can also be widely applied to safety monitoring of the dynamic operation of giant construction machinery.

## 1. Introduction

High-rise building machines (HBMs) are widely used as jack-up work platforms for the construction of super-high skyscrapers [1–3], such as the Shanghai Tower (632 m), Canton Tower (600 m), and other high-rise concrete core tubes [4, 5]. The HBM is a mobile construction platform that carries various construction equipment and facilities, such as tower cranes and concrete distributors, to large heights, thereby significantly increasing the construction efficiency of super-high buildings [6]. However, there are significant safety risks during the climbing stage of the HBM, and it is imperative to ensure stability. In particular, the attitude of the platform system while climbing is a critical control element during construction. Many aspects, including proper settings of safety evaluation and early warning indices for the HBM operation attitude, improving sensitivity and accuracy during

the climbing stage, and effectively monitoring the orientation during the climbing stage, are essential for mastering the real-time performance of the HBM and for minimizing safety risks.

Several studies have been conducted to examine construction safety risks and monitor equipment and facilities at construction sites [7–11]. Peng et al. [12] concluded that in their entire life cycle, buildings are prone to risks during the construction phase, particularly the concrete pouring phase of the reinforced concrete structures. Aneziris et al. [13] developed a quantitative model of occupational risk for construction workers and concluded that workers installing timber formworks have the highest risk of death. Luo et al. [14] attributed the high hazard rate at construction sites to the dynamic and complex characteristics of construction-related entities, such as the movement of construction equipment and workers and their interactions with each other. It is

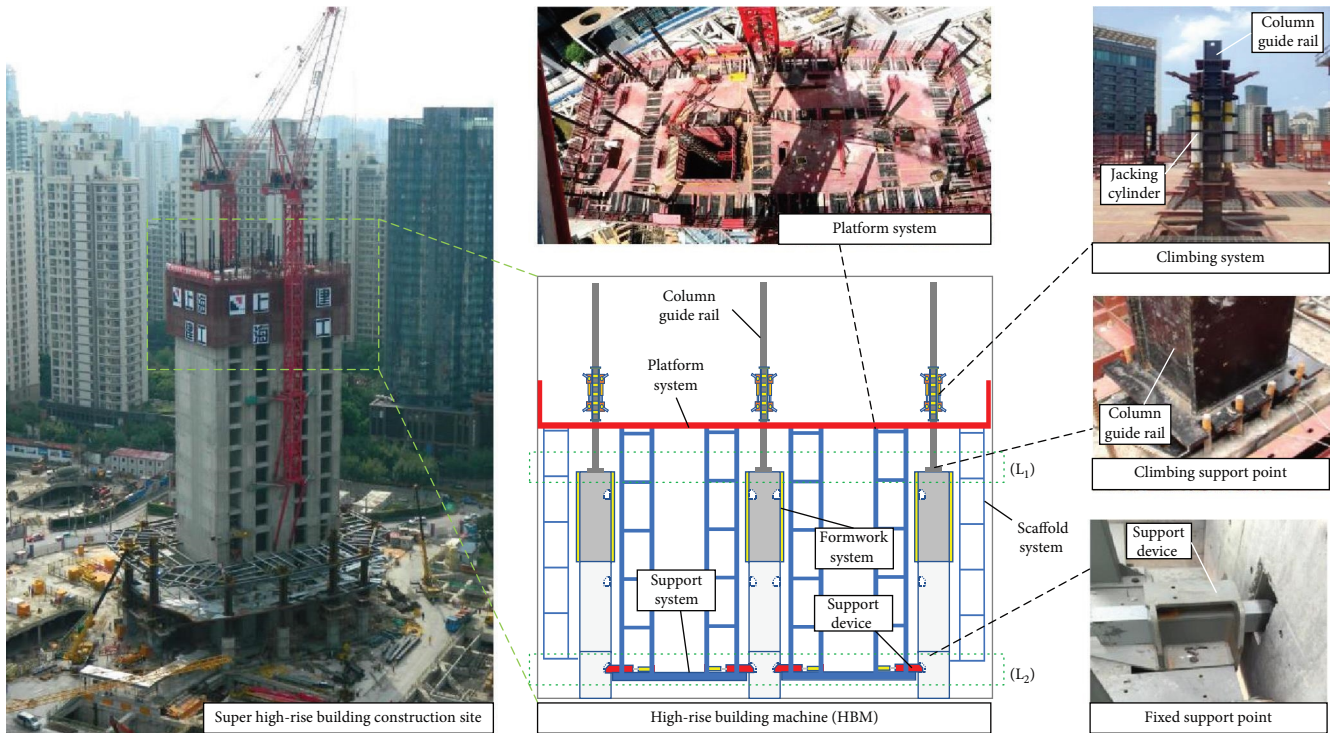


FIGURE 1: Structural composition of the HBM.

important to track the location, posture, and movement of construction equipment. Sherafat et al. [15] studied the feasibility of implementing various technical and computational techniques for the automatic activity identification and tracking of construction equipment and workers. Adam et al. [16] concluded that the risk of falling from heights is considerably high during the formwork construction phase of floor slabs and proposed prevention strategies and organizational methods to reduce the number of accidents during the formwork phase of floor slabs. Lim et al. [17] focused on system scaffolding, which is widely used at construction sites and developed a computer vision-based monitoring system for safety ropes and hooks to prevent fallings. Liu et al. [18] analyzed the main risk factors in the construction of a hydraulic self-climbing formwork. They concluded that significant safety risks are present in the operation of a hydraulic climbing formwork, especially during installation, dismantling, and position adjustment. These processes are prone to template collapse, falls from high places, and striking against objects. Zhang et al. [19] used a deep learning-based approach for the action recognition of excavators and dump trucks at construction sites. Rao et al. [20] identified the automated monitoring of construction sites as a significant research challenge and provided a comprehensive review of recent research on the real-time monitoring of construction projects. Zhang et al. [21] used accident causation theory and a systems thinking approach to construct a causation system model for construction accidents and conducted a case analysis of a particularly significant collapse safety accident that occurred in the Fengcheng Power Plant Project. Golafshani and Talatahari [22] analyzed the factors influencing the climbing rate of a slip

formwork system and concluded that weather conditions and operating height are important factors affecting the ascent rate of slip formwork systems. Montonen et al. [23] investigated a slew-control application for tower cranes to reduce the number of payload oscillations. Lee and Kim [24] developed a construction hoist control system supported by deep reinforcement learning to improve the efficiency of construction hoist operations. Yoon et al. [25] developed a dynamic simulator for mobile cranes based on the analyzed overturning limit data and applied analysis results to on-site tests. Shen et al. [26] proposed a four-level warning index based on risk management by combining the deformation development characteristics of an integral steel platform formwork. Zuo et al. [5] proposed a real-time remote monitoring system to determine the strength of concrete to accomplish safe climbing of the HBM.

The life cycle of HBM construction includes four stages: installation, climbing, operation, and dismantling [4]. Risks are mainly concentrated in the climbing and operating stages. Most existing studies have focused on the selection of a formwork system [27–29], performance analysis [30–32], and operational assessment [33, 34]. However, research on the dynamic analysis and control of the climbing stage of the HBM and its early warning indices is lacking.

## 2. Preliminaries

**2.1. Introduction of HBM.** The HBM is designed, in construction, as a bearing platform for large machinery and equipment. The HBM, as shown in Figure 1, consists of a platform system, scaffolding system, support system, climbing system, and formwork system.

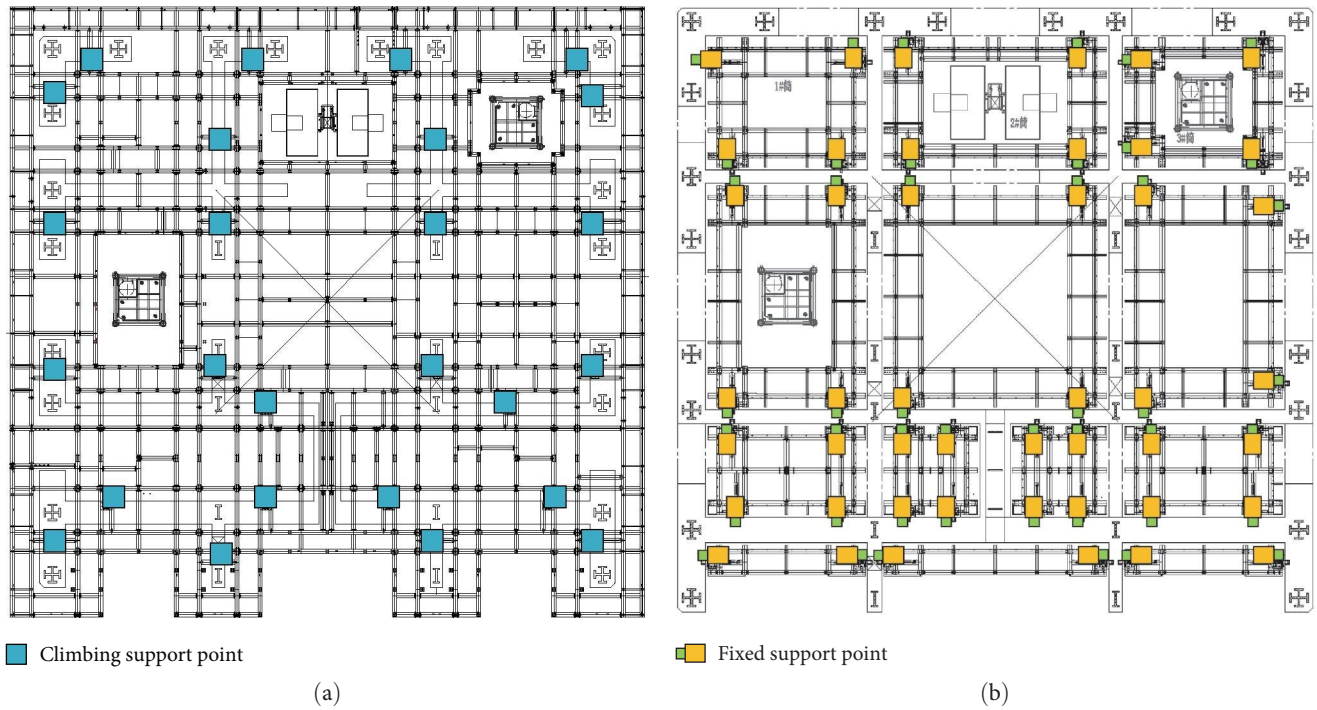


FIGURE 2: Distribution of (a) climbing support points and (b) fixed support points.

The platform system, located at the top of the core tube, forms a climbing operational community with the other four connected parts. They are composed of longitudinally and transversely distributed steel beams enclosed by steel sheets on their upper surfaces. The platform serves as a workspace for construction activities, accommodates equipment and materials, and distributes the loads to the support system. The support system connected below the platform system is the primary vertical force transmission system of the HBM. It uses support devices to transmit vertical and horizontal loads to concrete structures. The climbing system, supported by column guide rails on top of the concrete wall, was driven by a dual-acting hydraulic power system using multiple jacking cylinders to move the HBM.

The HBM is characterized by extensive coverage, size, and support points. The platform system is the primary bearing-plane layer among the HBM components, which makes it crucial for maintaining the construction stability of the HBM by controlling the platform system level during the climbing and operation stages.

During the operation stage, the HBM maintains a stable supporting state on the concrete via the support devices. However, during the climbing stage, the HBM and its associated equipment ascend vertically along the column guide rails, rendering the overall stability vulnerable to the climbing attitude. The horizontality of a platform system is a significant indicator of its overall stability. The factors affecting horizontality include the telescopic synchronization of each jacking cylinder and the height difference between each support point. The telescopic synchronization of the jacking cylinder can be regulated by programming the allowable displacement deviation value of the adjacent cylinder in a

programmable logic controller system. Support points are established primarily through the artificial setting of reserved holes or embedded parts in a concrete wall. However, achieving precise elevation control on the same floor is challenging and may result in height differences between the support points during construction, ultimately affecting the climbing attitude of the platform system.

Therefore, the support points can be divided into two types, climbing support points and fixed support points, which are evenly distributed in the plane position of the concrete structure. Figure 2 shows the distribution of the climbing and fixed support points in a typical project corresponding to layers  $L_1$  and  $L_2$ , as shown in Figure 1, respectively. The fixed support points primarily affect the initial and in-position attitudes of the HBM before and after climbing. In contrast, the climbing support point has a continual effect on the support capacity and overall stability of the platform system during ascent.

*2.2. Influence of Displacement Differences on Climbing.* Figure 3 shows the displacement differences in the platform system resulting from the asynchronous climbing of climbing systems  $a$ ,  $b$ , and  $c$  during the climbing stage. The displacement differences between corresponding positions of the platform system are represented by  $\Delta h_{ab}$ ,  $\Delta h_{ac}$ , and  $\Delta h_{bc}$ . These values are dynamic and change in real time throughout the climbing process.

$\Delta h_0$  refers to the maximum vertical difference of the platform system due to the height difference of the fixed support points ( $\Delta h_{L2}$ ) before climbing, as shown in Figure 3(a). This value varies between the structural floors of the building but remains relatively constant during the climbing process of



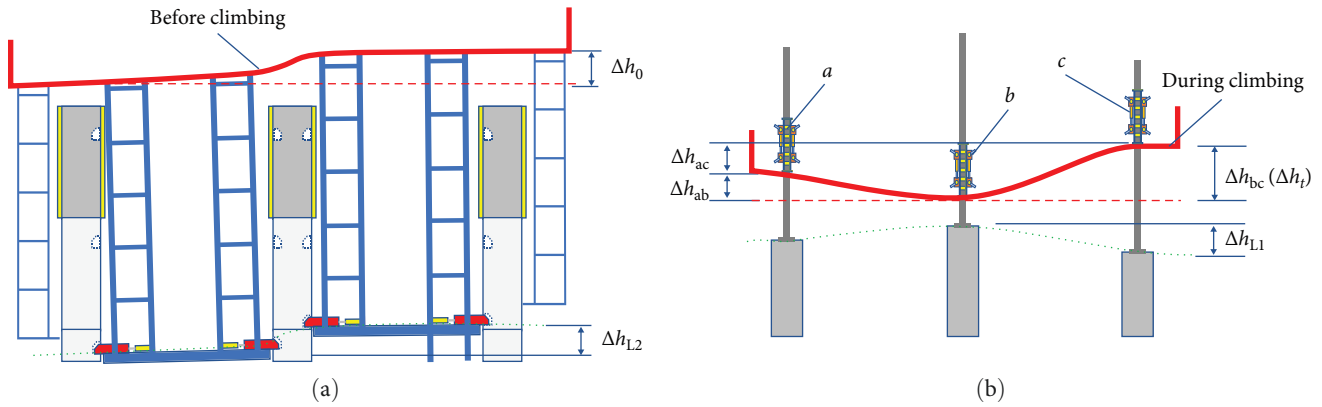


FIGURE 3: Principle diagram of the vertical deformation of the platform system: (a) before climbing; (b) during climbing.

each floor. Furthermore, the measurements obtained by the monitoring points on the platform system comprise both the asynchronous vertical displacement during climbing and the height difference of the fixed support points.

In each climbing stage, the height difference of the climbing support point ( $\Delta h_{L1}$ ) determines the initial height of each jacking cylinder on the guide rail. The operator's primary concern is the real-time change of the maximum displacement difference,  $\Delta h_t$ , which is the maximum value of  $\Delta h_{ab}$ ,  $\Delta h_{ac}$ , and  $\Delta h_{bc}$ , as shown in Figure 3(b). However, the interference of  $\Delta h_0$  needs to be addressed to enable the operator to precisely control the real-time climbing attitude of the platform system.

### 3. Methodology

The difference in the displacement between the support points can affect the initial and climbing stages of the HBM before each climb. Therefore, if the warning threshold remains fixed during the climbing process, the attitude changes in the entire platform system cannot be accurately identified. This study proposes a monitoring and early warning method to accurately control the real-time attitude of an HBM during the climbing stage. Figure 4 shows a flowchart of the proposed method. The approach begins with the determination of a monitoring program based on specific construction requirements. Subsequently, real-time monitoring values from multiple sensors are utilized to correct the impact of the support points. This method comprises three main steps as described below.

**3.1. Identifying Monitoring Points.** The monitoring point was set on the main bearing steel beam of the platform system, close to the point of intersection of the longitudinal and transverse beams. The monitoring points were evenly distributed on the steel platform. The more the number of monitoring points deployed, the more finely the real-time state of the platform system can be sensed. However, considering the economy and operability, a monitoring point can be arranged at key positions with a spacing of 5–10 m. For a rectangular platform system, it should be noted that no less than five level sensors were distributed on the main stress

plane of the HBM, no less than one level sensor was set in the central position, and the four corners of the main stress plane. The total number of leveling sensors was  $m \geq 5$ .

Figure 5 shows the layout of the monitoring points on the platform plane. Monitoring points were arranged during the first installation of the HBM. The height of each monitoring point should be consistent and determined at the same horizontal position such that the height difference measured by the monitoring points can represent the vertical deformation of the steel platform.

**3.2. Arranging Monitoring Sensors.** To monitor the working behavior of the HBM in real time, multiple monitoring points were distributed in the platform system, and monitoring sensors were installed at each monitoring point to collect the vertical displacement and offset data of the point in real time and send it to the monitoring system. The monitoring sensor used a fiber grating static leveler with good transmission stability, which was less affected by external interference and provided accurate data (see Figure 6). All the sensors were mounted on the web of the steel beam at the same elevation in the platform system to ensure that the baseline readings for each level were identical. The fiber grating static level operates based on the principle of liquid connectivity, in which multiple liquid storage tanks are linked through pipes to maintain an equal liquid level. Liquid-level sensors measure the height of the liquid in different storage tanks. The relative difference in the vertical displacement ( $H_1 - H_4$ , as shown in Figure 6) for each static level is calculated based on these data, making it well-suited for precisely monitoring vertical displacement. Table 1 lists the main parameters of the fiber grating static level sensor.

### 3.3. Dynamic Monitoring and Early Warning

**3.3.1. Dynamic Monitoring.** Prior to the climbing stage, a predetermined time interval  $\Delta t$  was allotted during which  $n$  readings were taken for each level at each moment.  $\Delta t$  represents a constant time interval within the operation stage; it can be specified as needed, typically not less than 60 s, and must occur before the ascent of the HBM. The maximum value  $H_{imax}$ , the minimum value  $H_{imin}$ , and the

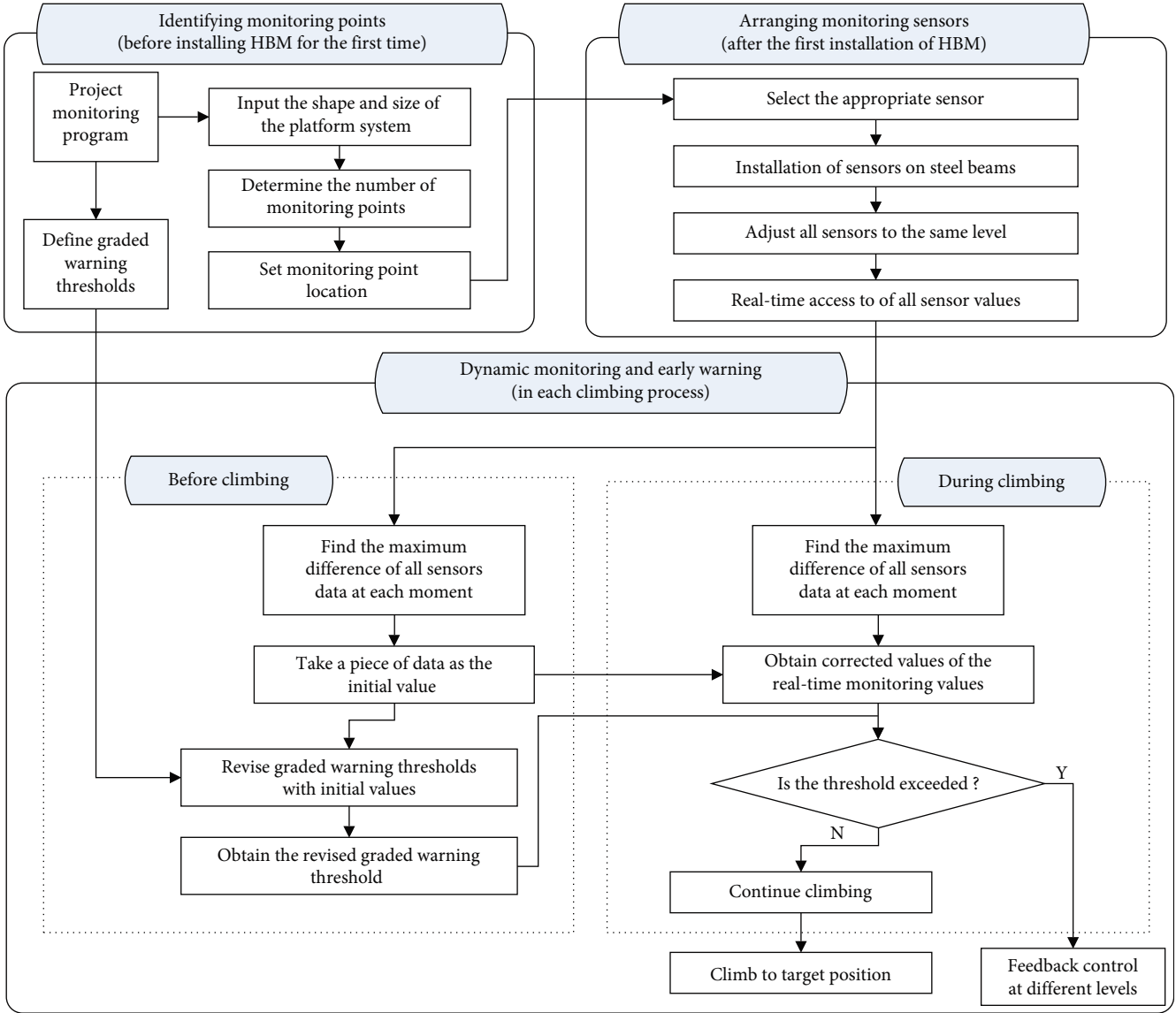


FIGURE 4: Monitoring and early warning method of climbing attitude for the HBM.

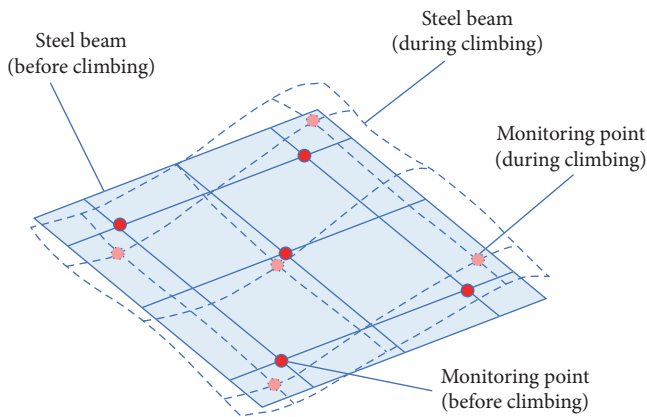


FIGURE 5: Layout of the monitoring points.

difference  $\Delta h_i$  between the measured values of all level sensors in the time period  $\Delta t$  were obtained, respectively, as follows:

$$H_{i\max} = \max\{H_{i1}, \dots, H_{im}\}, \quad (1)$$

$$H_{i\min} = \min\{H_{i1}, \dots, H_{im}\}, \quad (2)$$

$$\Delta h_i = H_{i\max} - H_{i\min}, \quad (3)$$

where  $m$  is the total number of level sensors,  $n$  is the total number of data measured by a single level sensor during  $\Delta t$ , and the integer  $i$  is within the range  $[1, n]$ .  $H_{i\max}$  and  $H_{i\min}$  are the maximum and minimum readings of all the level sensors at a specific point within  $\Delta t$ , respectively. Additionally,  $\Delta h_i$  is

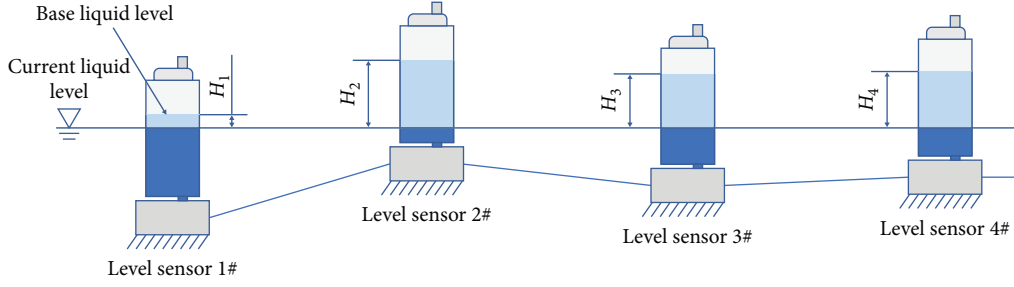


FIGURE 6: Technical principle diagram of the level sensor.

TABLE 1: Main parameters of the level sensor.

Item	Parameters
Standard range	0–100 mm
Measurement accuracy	<0.3% FS
Wavelength range	1,500–1,590 nm
Protection level	IP67
Working environment	–40 to +120°C

the maximum displacement difference of all level sensors at a point in  $\Delta t$ .

Significant deviations in the overall data might occur due to defects in individual data; to prevent this, the value of  $\Delta h_0$  was calculated by taking the geometric mean of  $\Delta h_i$ .

$$\Delta h_0 = \sqrt[n]{\prod_{i=1}^n \Delta h_i}. \quad (4)$$

During the climbing stage, each sensor monitors the real-time vertical displacement of its own point and sends this information to a monitoring system. To obtain the maximum measured value of the maximum displacement difference at the current moment, the maximum value  $H_{t_{\max}}$ , the minimum value  $H_{t_{\min}}$ , and the difference between them  $\Delta h_t$  can be determined as follows:

$$H_{t_{\max}} = \max\{H_{t1}, \dots, H_{tm}\}, \quad (5)$$

$$H_{t_{\min}} = \min\{H_{t1}, \dots, H_{tm}\}, \quad (6)$$

$$\Delta h_t = H_{t_{\max}} - H_{t_{\min}}, \quad (7)$$

where  $H_{t_{\max}}$  and  $H_{t_{\min}}$  are the maximum and minimum values of all the level sensors at time  $t$ , respectively, and  $\Delta h_t$  is the maximum measured displacement of all the level sensors at time  $t$  in the climbing process.

Hence, the levelness of the platform system can be monitored dynamically in real time. As a result, this can reflect whether the jacking speed of the climbing cylinders is synchronized.

**3.3.2. Early Warning.** In the climbing stage, corrections are made to  $\Delta h_t$  and  $f_h$  using the initial values of the current phase, which provide  $\Delta h'_t$  and  $f'_h$ , respectively. The graded

scale factor  $\mu$  is employed to determine the early warning threshold  $X$ .

$$\Delta h'_t = |\Delta h_t - \Delta h_0|, \quad (8)$$

$$f_h = \alpha L, \quad (9)$$

$$f'_h = f_h - \Delta h_0, \quad (10)$$

$$X = \mu f'_h, \quad (11)$$

where  $\Delta h'_t$  is the maximum displacement difference correction value of all level sensors at the current moment in the climbing process, and  $f_h$  is the maximum displacement difference warning value. For a rectangular platform system,  $L$  is the length of the long side of the platform system plane, and for a circular steel platform,  $L$  is the diameter of the platform system plane.  $\alpha$  is the scale factor, which is based on the control requirements of the actual construction project. According to the practical results of several super high-rise building monitoring projects, 2‰ of the maximum side length  $L$  of the platform system plane was considered as the maximum warning control value for test verification [35].  $f'_h$  is the corrected maximum displacement difference warning value,  $\mu$  is the graded scale factor of the warning control value, and  $X$  is the early warning threshold of the current climbing stage. In a typical three-level warning system, the values of  $\mu$  are taken as 50%, 80%, and 100%. Therefore,  $X_1$ ,  $X_2$ , and  $X_3$  correspond to the first-, second-, and third-level warning thresholds, respectively.

The variable  $\Delta h'_t$  serves as a basis for comparing with  $X$  and determining the appropriate warning interval. Throughout the ascent,  $\Delta h'_t$  remains in a designated location and generates graded warning feedback as necessary. The HBM safety warning control value, grading rules, and feedback measures can be set based on the results of the structural analysis of the project, relevant standards and specifications, special construction programs, and specific requirements for project site control. The grading of monitoring levels should not only meet the needs of the recognition degree of structural working conditions, but also comprehensively control the structural working conditions. However, it should not be graded excessively, as it does not suit the actual operation.



FIGURE 7: Deployment of level sensors for the HBM in the Shenzhen Xinghe Yabao Building.

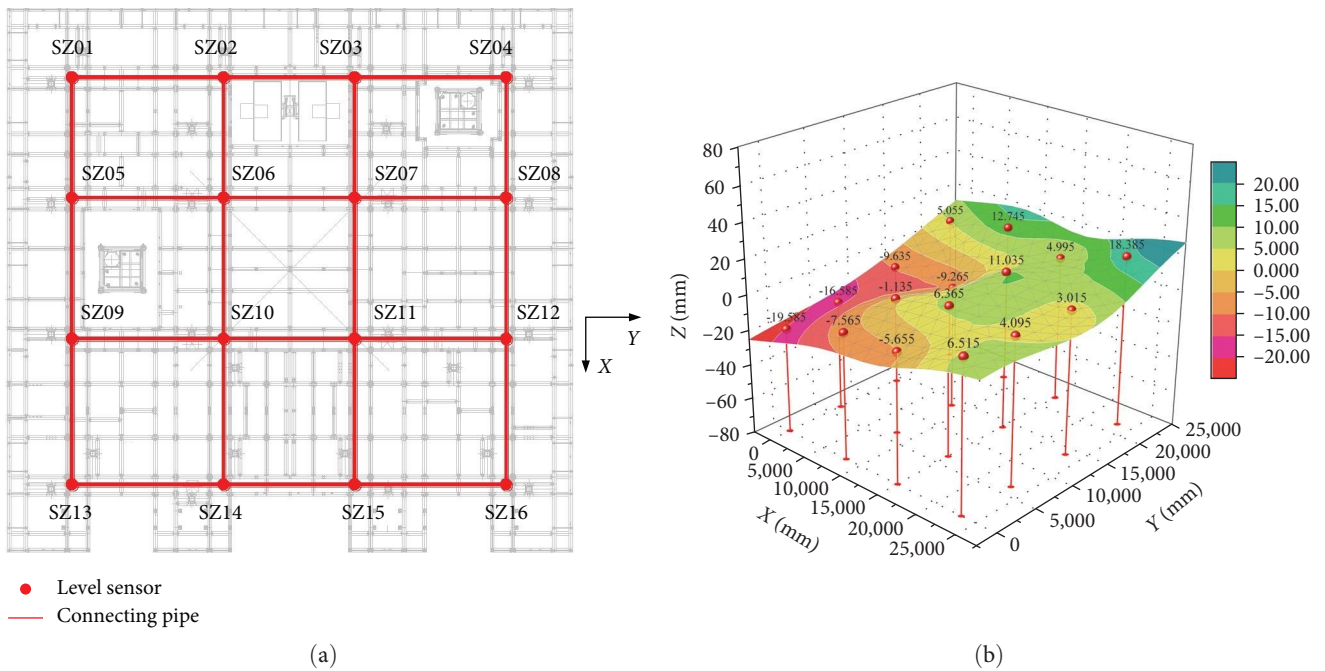


FIGURE 8: Level sensor arrangement and measured values: (a) level sensor arrangement diagram; (b) cloud plot of typical measured values before a single climb.

### 4. Case Study

**4.1. Project Overview.** The west tower of the super-high-rise project of Shenzhen Xinghe Yabao Building is 356 m in height, 74 stories above ground, and 4.5 m in standard floor height. The core tube of the tower is rectangular, and the tube size is 27.40 × 26.15 m. The concrete core tube structure of the tower was constructed using an HBM (Figure 7). The plane size of the platform system was 30.20 × 28.95 m. This HBM had 26 climbing systems and 46 fixed support points, and it takes ~2 hr to complete one climb of 4.5 m. According to the project schedule, an average of one climb per week was required.

**4.2. Identifying Monitoring Points and Arranging Monitoring Sensors.** To monitor the levelness of the HBM in real time, 16 level sensors were setup at the steel beam position of the main force plane of the platform system, including four points at the center and 12 points around it (Figure 7). After the initial installation, all the sensors were calibrated to ensure that they were at the same level and read “0.” The sensors were numbered from SZ1 to SZ16, and their positions are shown in Figure 8(a). Figure 8(b) shows the measured values of the 16 monitoring points at a given time before climbing. The highest and lowest points are located in the diagonal positions of the platform system, and it was observed that sensor SZ1 recorded the lowest reading at



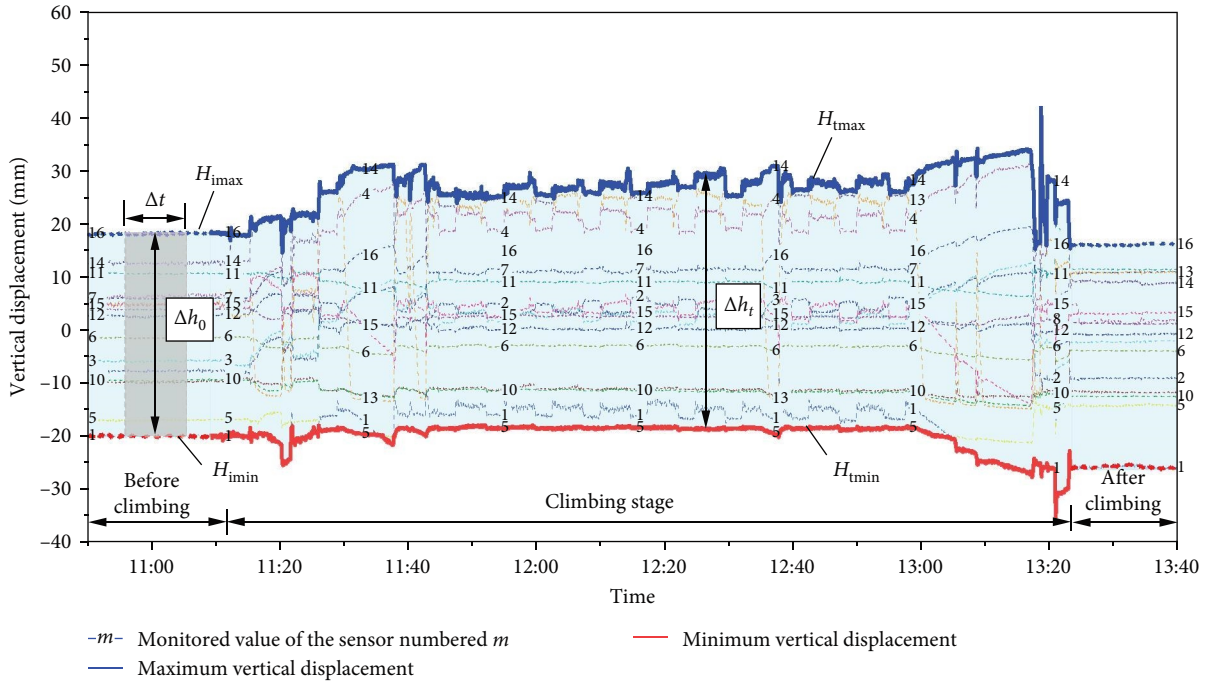


FIGURE 9: Vertical displacement monitoring values at different times for a climbing process using level sensors.

−19.58 mm, while sensor SZ16 recorded the highest reading at 18.39 mm.

The real-time readings of the 16 sensors indicate that the platform system underwent some degree of tilt after multiple climbs, as it differed from the horizontal state recorded just after the initial installation. The platform system position at the location of sensor SZ1 was lower, while the position of the platform system at the location of sensor SZ16 was higher. Before climbing the HBM, the material load at the top was cleared, thereby eliminating uneven load issues. Therefore, the platform system tilt was mainly attributed to the uneven support displacement difference at the bottom caused by the inaccuracy in setting the support points during the previous climbs.

#### 4.3. Dynamic Monitoring and Early Warning

**4.3.1. Dynamic Monitoring.** Figure 9 shows the measured time history data of 16 level sensors during a climbing process. The graph shows that before 11:10, the 16 sensors had different readings in the range (−20,20) due to variations in the height of the fixed support points of the HBM. Despite these differences, the HBM remained in a stable support condition and the readings remained relatively constant. From 11:10 to 11:43, the fixed support points of the HBM gradually changed to climbing support points, causing significant changes in the levelness of the platform and redistributing the height differences between the 16 sensors until all support points had completed the transition. Subsequently, the HBM entered a stable climbing state and the readings gradually stabilized. At 13:00, the HBM reached its target height but required another transition from climbing to the fixed support points, causing significant changes in the readings of the 16 sensors until completion at 13:25. The entire

climbing process took 2 hr and 15 min. After completion, the fixed support points of the HBM extended into the next structural layer, resulting in a stable support condition, but with different height differences, resulting in a measurement range (−25,15). This indicates that the variation in  $\Delta h_0$  can be attributed to the height differences between the fixed support points in different structural layers, and that the measured value of each level sensor during the climbing stage exhibited a greater degree of fluctuation as compared to the operation stage.

Figure 10 shows the time history data of the measured value  $\Delta h_t$  of the three consecutive climbing processes, i.e., the climbing process, as shown in Figure 9, followed by two consecutive climbing processes. There was an interval of approximately 6 days between each climbing process. Because there was a displacement difference between the fixed support points before and after each climb, the maximum displacement difference at the starting and ending positions exhibited a step-like feature. Such a step-like horizontal displacement difference does not contribute to a precise evaluation of the state of the HBM during the climbing process.

For the three processes, the actual value of the level sensor was taken 30 min before climbing,  $\Delta t = 1,800$  s, and the values of  $\Delta h_0$  can be calculated using Equations (1)–(4) and were found to be 37.9, 41.6, and 34.7 mm, respectively. Real-time data of  $\Delta h_t$  can then be obtained during the climbing process using Equations (5)–(7), which serve as a monitoring indicator of the HBM level.

**4.3.2. Early Warning.** According to Equation (9),  $L = 30.20$  m and  $\alpha = 0.002$ ; thus, the maximum displacement warning value  $f_h = 60.4$  mm is obtained for the HBM. To accurately control the status of the HBM, three levels of



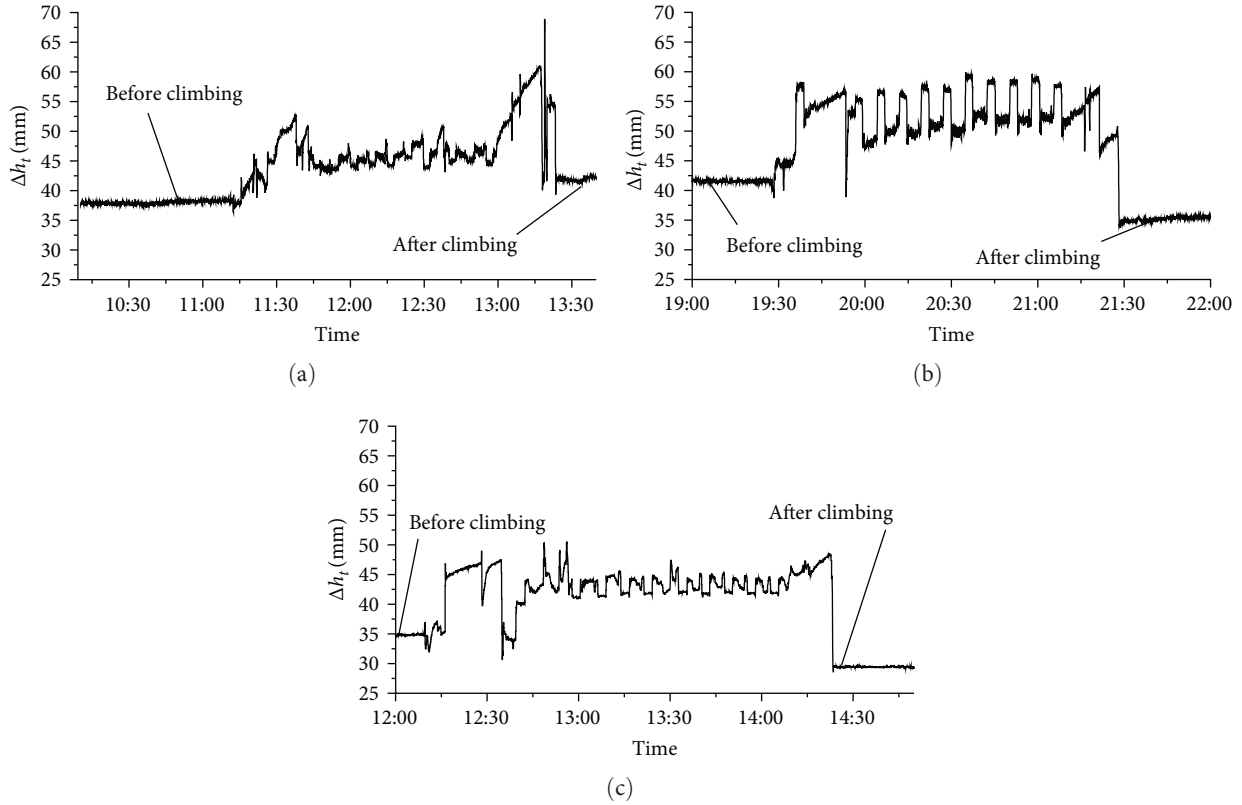


FIGURE 10: Comparison of the measured time range data of the level sensor for three consecutive climbs: (a) climbing process 1; (b) climbing process 2; (c) climbing process 3.

TABLE 2: Warning level and feedback method for HBM.

Item	First level	Second level	Third level
Early warning threshold $X$			
Climbing process 1	11.3 mm	18.0 mm	22.5 mm
Climbing process 2	9.4 mm	15.1 mm	18.8 mm
Climbing process 3	12.8 mm	20.5 mm	25.7 mm
Graded scale factor $\mu$	50%	80%	100%
Feedback method	Highlight labeling	Sound and light warning	Shutdown and check

warning values were setup. Fifty percent, 80%, and 100% of the maximum displacement difference warning value were taken as the graded scale factor  $\mu$  of the first, second, and third level warning intervals, respectively.

It can be observed here that if a fixed warning threshold is adopted, the initial difference interferes with the changed behavior in the climbing process. For example, the benchmark warning values of the platform system climbing level in this project were 30.2, 48.3, and 60.4 mm, respectively. The initial displacement difference of the three climbs, as shown in Figure 10, is higher than the first-level threshold of 30.2 mm. Therefore, it is easy to trigger and remain in the first-level alarm state for a long time during the climbing process, thereby reducing the sensitivity of the operator to changes in height difference during the climbing process.

$f'_h$  and  $X$  were calculated using Equations (10) and (11), respectively. Table 2 lists the warning levels and corresponding

feedback methods for the HBM during the three climbing processes mentioned above.

During the climbing process, the correction value of maximum displacement  $\Delta h'_i$  of all level sensors at the current moment was calculated using Equations (5)–(8) and compared with  $X_1$ ,  $X_2$ , and  $X_3$ . When the measured values exceeded the early warning threshold, corresponding feedback measures were issued.

Figure 11 shows the corrected measured values and the application of graded warnings during the climbing stage. As seen in climbing process 1 (Figure 11(a)),  $\Delta h'_i$  of the platform system varies greatly during the climbing stage, especially in the initial and conversion phases, while the variation is relatively small in the stable climbing phase. During the final conversion phase, the  $\Delta h'_i$  continued to increase and exceeded the warning threshold  $X_3$  at 13:13, resulting in manual intervention to briefly produce a large change in the height

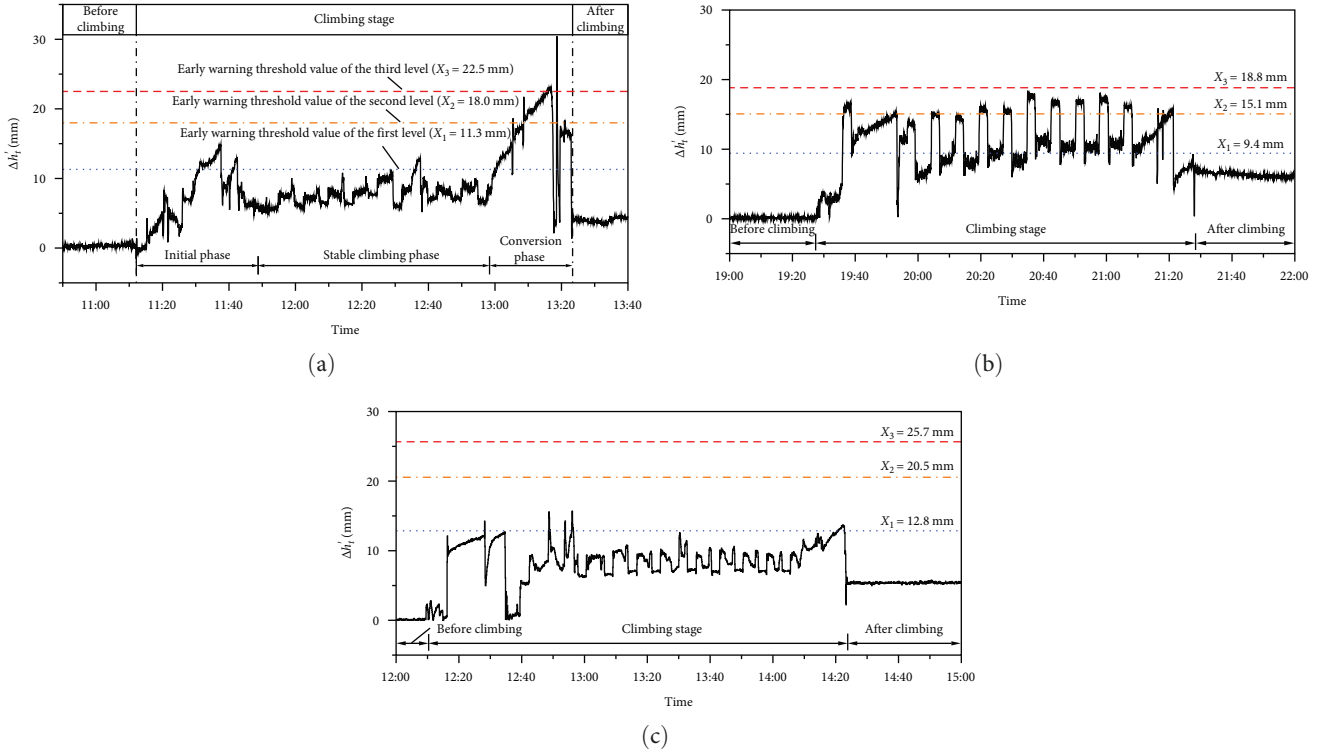


FIGURE 11: Corrected measured values and the application of graded warnings: (a) climbing process 1; (b) climbing process 2; (c) climbing process 3.

difference. However, it quickly returned to a value within warning threshold  $X_2$  and returned to normal levels after the support was in place.

Both climbing processes remained below the maximum warning threshold  $X_3$ . However, the  $\Delta h_0$  of climbing process 2 (Figure 11(b)) was higher at 41.6 mm, resulting in a smaller margin of displacement difference during its climb and several instances of exceeding the second warning threshold  $X_2$ . In contrast, climbing process 3 (Figure 11(c)) had a relatively small  $\Delta h_0$  at 34.7 mm and was smoother overall, indicating a better climbing stage. By comparing climbing processes 2 and 3, we can infer that when the overall size of the HBM is determined,  $f_h$  becomes constant. Therefore, as  $\Delta h_0$  increases,  $f'_h$  decreases, and the likelihood of  $\Delta h'_t$  exceeding the warning threshold increases. Accordingly, the climbing process requires higher corresponding attitude control.

Therefore, the larger the  $\Delta h_0$ , the more unbalanced the attitude of HBM, resulting in a smaller surplus of attitude control during the climbing process, making  $X_1$ ,  $X_2$ , and  $X_3$  closer together, which can cause the attitude of the platform to exceed the warning threshold due to the slight asynchronicity of the climbing cylinder. Furthermore, in all three climbing processes,  $\Delta h_0$  was greater than  $X_3$ , indicating that the presence of initial height differences has a significant impact on the climbing attitude of the HBM.

## 5. Discussion

In this study, we proposed a monitoring and early warning method for HBMs during climbing to monitor the climbing

of large construction equipment. We studied in detail the influences of the displacement difference of the support points on the climbing phase and used the initial value before each climbing stage to correct the current warning classification indexes and real-time monitoring values. In addition, we used the geometric mean for preclimb sampling, which improved the accuracy of the initial value as compared to the direct monitoring of a single time point value. This method can improve the sensitivity to small changes in the climbing process, thus more finely monitoring the climbing attitude of large integral structures. Existing monitoring methods focus on the state of the climbing system components, such as the climbing rate of the equipment [22], safety of the support points [5], and do not monitor the climbing attitude of the entire equipment. In addition, warning classification indices are usually fixed and do not consider the influence of the deviation of the support points on each structural floor, lacking a revision for each climbing process [26].

The case study shows that, when the overall HBM attitude control is constrained, the initial displacement difference of the support points before climbing significantly affects the climbing attitude. By enhancing the precision of the manual setting of the embedded parts and support points at each structural layer, the warning threshold during the climbing process can be increased, making it easier to control the safety state of the HBM. Hence, replacing manual construction with mechanized and automated technologies is an effective approach for improving the safety of HBM during climbing.

The proposed method achieves satisfactory results in practice. It improved the assessment of the HBM working posture during climbing, promoted the timely identification and resolution of problems, and allowed operators and managers to better control the working conditions to ensure construction safety. This method can be used for HBM and other climbing equipment, such as hydraulic self-climbing [18] and slip formwork systems [22].

However, this study has some limitations. First, we considered the climbing deformation of the main bearing layer of this equipment from the viewpoint of economy and operability and did not comprehensively monitor the climbing attitude of other structures, such as the scaffold, support, and climbing systems. Second, in the main bearing layer, only the deformation of several points was monitored using this method, and the monitoring object did not include the steel beams.

Therefore, a more accurate method is required to monitor climbing equipment. Various types of sensors (e.g., cameras and laser ranging sensors) can be added to the acquisition and analysis system to further improve accuracy, and data fitting can be used to identify the spatial relationship between two monitoring points. In addition, the deep learning approach can be considered in future studies on construction equipment safety management [36], such as predicting the motion attitude of climbing equipment by accumulating a large amount of climbing data.

## 6. Conclusions

- (1) The climbing stability of the HBM was affected by unsynchronized climbing systems and differential displacements of the support points. The synchronization of the climbing system is a key factor in monitoring the climbing of giant HBM. The displacement differences at the support points primarily affected the initial conditions before each climb. Thus, the differential displacements and synchronization of the climbing system should be thoroughly evaluated to enhance the overall climbing stability of the HBM.
- (2) During the HBM climbing stage, the primary focus is on the horizontal monitoring and warning of the main load-bearing plane. Therefore, level-sensor monitoring points can be setup in the distribution of the main force plane according to the size of the HBM, and the maximum displacement difference can be used as a discriminant index of the climbing attitude of the HBM. The attitude of the HBM was then controlled in real time by setting three-level warning thresholds to achieve dynamic identification and early warning. This method achieved good results in practice, ensuring the safety of giant HBMs and providing continuous and efficient management of the construction process.
- (3) The differential displacement at the construction site could be attributed to the inaccuracy of manually setting the support positions. The larger the support point displacement difference, the smaller the warning

threshold during climbing. Therefore, it is recommended that mechanized construction and refined monitoring methods can be adopted to replace manual labor, improve construction accuracy, and facilitate control over the HBM climbing process, thereby making construction activities safer and more efficient.

## Data Availability

The datasets used in this study are available from the corresponding author upon reasonable request.

## Conflicts of Interest

The authors declare that they have no conflicts of interest.

## Acknowledgments

This research was supported by National Key R&D Program of China (No. 2022YFC3802200) and Shanghai Enterprise Innovation Development and Capacity Enhancement Project (No. 2022007).

## References

- [1] T. Wakisaka, N. Furuya, Y. Inoue, and T. Shiokawa, "Automated construction system for high-rise reinforced concrete buildings," *Automation in Construction*, vol. 9, no. 3, pp. 229–250, 2000.
- [2] Y. Ikeda and T. Harada, "Application of the automated building construction system using the conventional construction method together," in *Proceedings of the 23rd ISARC*, pp. 722–727, Tokyo, Japan, October 2006.
- [3] T. Bock and T. Linner, *Site Automation: Automated/Robotic on-Site Factories*, Cambridge University Press, New York, USA, 2016.
- [4] J. Gong, *Technology of Integrated Climbing Scaffolding and Formwork System Including Steel Platform for Construction of Super High Rise Structures*, China Architecture & Building Press, Beijing, China, in Chinese, 2018.
- [5] Z. Zuo, Y. Huang, X. Pan et al., "Experimental research on remote real-time monitoring of concrete strength for highrise building machine during construction," *Measurement*, vol. 178, Article ID 109430, 2021.
- [6] J. Gong, T. Fang, and J. Zuo, "A review of key technologies development of super high-rise building construction in China," *Advances in Civil Engineering*, vol. 2022, Article ID 5438917, 13 pages, 2022.
- [7] Y. Shen, M. Xu, Y. Lin, C. Cui, X. Shi, and Y. Liu, "Safety risk management of prefabricated building construction based on ontology technology in the BIM environment," *Buildings*, vol. 12, no. 6, Article ID 765, 2022.
- [8] C. P. Pham, P. T. Nguyen, P. T. Phan, Q. L. H. T. T. Nguyen, L. P. Le, and M. T. H. Duong, "Risk factors affecting equipment management in construction firms," *The Journal of Asian Finance, Economics and Business*, vol. 7, no. 11, pp. 347–356, 2020.
- [9] T. Chinda and P. Pongsayaporn, "Relationships among factors affecting construction safety equipment selection: structural equation modelling approach," *Civil Engineering and Environmental Systems*, vol. 37, no. 1-2, pp. 28–47, 2020.
- [10] Z. He, M. Gao, T. Liang, Y. Lu, X. Lai, and F. Pan, "Tornado-affected safety assessment of tower cranes outer-attached to



- super high-rise buildings in construction,” *Journal of Building Engineering*, vol. 51, Article ID 104320, 2022.
- [11] L. Jiang, T. Zhao, W. Zhang, and J. Hu, “System hazard analysis of tower crane in different phases on construction site,” *Advances in Civil Engineering*, vol. 2021, Article ID 7026789, 16 pages, 2021.
- [12] J. L. Peng, A. D. Pan, D. V. Rosowsky, W. F. Chen, T. Yen, and S. L. Chan, “High clearance scaffold systems during construction—I. Structural modelling and modes of failure,” *Engineering Structures*, vol. 18, no. 3, pp. 247–257, 1996.
- [13] O. N. Aneziris, E. Topali, and I. A. Papazoglou, “Occupational risk of building construction,” *Reliability Engineering & System Safety*, vol. 105, pp. 36–46, 2012.
- [14] H. Luo, M. Wang, P. K.-Y. Wong, and J. C. P. Cheng, “Full body pose estimation of construction equipment using computer vision and deep learning techniques,” *Automation in Construction*, vol. 110, Article ID 103016, 2020.
- [15] B. Sherafat, C. R. Ahn, R. Akhavian et al., “Automated methods for activity recognition of construction workers and equipment: state-of-the-art review,” *Journal of Construction Engineering and Management*, vol. 146, no. 6, Article ID 03120002, 2020.
- [16] J. M. Adam, F. J. Pallarés, and P. A. Calderón, “Falls from height during the floor slab formwork of buildings: current situation in Spain,” *Journal of Safety Research*, vol. 40, no. 4, pp. 293–299, 2009.
- [17] J. Lim, D. G. Jung, C. Park, and D. Y. Kim, “Computer vision process development regarding worker’s safety harness and hook to prevent fall accidents: focused on system scaffolds in South Korea,” *Advances in Civil Engineering*, vol. 2022, Article ID 4678479, 12 pages, 2022.
- [18] X. Liu, Y. Hu, D. Chen, and L. Wang, “Safety control of hydraulic self-climbing formwork in south tower construction of Taizhou bridge,” *Procedia Engineering*, vol. 45, pp. 248–252, 2012.
- [19] J. Zhang, L. Zi, Y. Hou, M. Wang, W. Jiang, and D. Deng, “A deep learning-based approach to enable action recognition for construction equipment,” *Advances in Civil Engineering*, vol. 2020, Article ID 8812928, 14 pages, 2020.
- [20] A. S. Rao, M. Radanovic, Y. Liu et al., “Real-time monitoring of construction sites: sensors, methods, and applications,” *Automation in Construction*, vol. 136, Article ID 104099, 2022.
- [21] W. Zhang, S. Zhu, X. Zhang, and T. Zhao, “Identification of critical causes of construction accidents in China using a model based on system thinking and case analysis,” *Safety Science*, vol. 121, pp. 606–618, 2020.
- [22] E. M. Golafshani and S. Talatahari, “Predicting the climbing rate of slip formwork systems using linear biogeography-based programming,” *Applied Soft Computing*, vol. 70, pp. 263–278, 2018.
- [23] J.-H. Montonen, N. Nevaranta, M. Niemelä, and T. Lindh, “Comparison of extrainsensitive input shaping and swing-angle-estimation-based slew control approaches for a tower crane,” *Applied Sciences*, vol. 12, no. 12, Article ID 5945, 2022.
- [24] D. Lee and M. Kim, “Autonomous construction hoist system based on deep reinforcement learning in high-rise building construction,” *Automation in Construction*, vol. 128, Article ID 103737, 2021.
- [25] B.-J. Yoon, K.-S. Lee, and J.-H. Lee, “Study on overturn proof monitoring system of mobile crane,” *Applied Sciences*, vol. 11, no. 15, Article ID 6819, 2021.
- [26] Y. Shen, L. Xu, and S. Wang, “Research on early-warning index for deformation of integrated scaffolding and formwork with steel platform based on risk management,” *Chinese, China Safety Science Journal*, vol. 31, no. 6, pp. 56–63, 2021.
- [27] A. Duran and N. Prašćević, “Allocation and selection of equipment for concrete works using fuzzy linear programming,” *Building Materials and Structures*, vol. 64, no. 3, pp. 195–199, 2021.
- [28] T. Terzioglu and G. Polat, “Formwork system selection in building construction projects using an integrated rough AHP-EDAS approach: a case study,” *Buildings*, vol. 12, no. 8, Article ID 1084, 2022.
- [29] T. Terzioglu, G. Polat, and H. Turkoglu, “Formwork system selection criteria for building construction projects: a structural equation modelling approach,” *Buildings*, vol. 12, no. 2, Article ID 204, 2022.
- [30] T. Craipeau, F. Toussaint, A. Perrot, and T. Lecompte, “Experimental approach on a moving formwork,” *Construction and Building Materials*, vol. 270, Article ID 121472, 2021.
- [31] J.-W. Xia, Y.-L. Yao, X.-S. Wu, and Y.-H. Chen, “Calculation and analysis of hydraulic automatic climbing formwork equipment for super-high building construction,” *Journal of the International Association for Shell and Spatial Structures*, vol. 62, no. 1, pp. 24–36, 2021.
- [32] S. Hu and J. Li, “Analysis of dynamic characteristics of climbing formwork under wind loads,” in *E3S Web of Conferences*, vol. 79, 2019.
- [33] M. R. Kannan and M. H. Santhi, “Constructability assessment of climbing formwork systems using building information modeling,” *Procedia Engineering*, vol. 64, pp. 1129–1138, 2013.
- [34] V. T. Nguyen, K. A. Nguyen, and V. L. Nguyen, “An improvement of a hydraulic self-climbing formwork,” *Archive of Mechanical Engineering*, vol. 66, no. 4, pp. 495–507, 2019.
- [35] JGJ 459-2019, “JGJ 459-2019, *Technical Standard for Self-Climbing Integrated Scaffolding and Formwork Equipment with Steel Platform*,” China Architecture & Building Press, Beijing, China, in Chinese, 2019.
- [36] H. T. T. L. Pham, M. Rafieizonooz, S. Han, and D. E. Lee, “Current status and future directions of deep learning applications for safety management in construction,” *Sustainability*, vol. 13, no. 24, Article ID 13579, 2021.